the reaction mixture was diluted with 14 ml of methylene chloride containing 5 mmol of the compound to be examined. This makes the mixture 1 M in hydride and 0.25 M in the compound under investigation. At appropriate time intervals, 2 ml of aliquots were withdrawn and quenched in a THF-glycerin-2 N HCl hydrolyzing mixture. The hydrogen evolved was measured volumetrically. For the reaction of compounds with active hydrogen, the hydrogen evolved was collected in a gas-buret and measured the volume of hydrogen.

The reaction of 2-heptanone is described as a representative procedure. A 100-ml oven-dried flask, equipped with a sidearm and a reflux condenser, connected to a gas-buret *via* a dry ice-acetone trap[5]. The flask was placed in an ice-water bath and cooled down under dry nitrogen. To this flask was added 6 ml of 3.34 M ThxBHBr solution in methylene chloride, and followed by addition of 14 ml of 2-heptanone (0.57g, 5 mmol) solution in methylene chloride. No hydrogen evolution was observed. After 1 h at 0°C, hydrolysis of a 2-ml aliquot of the reaction mixture indicated 1.70 mmol of residual hydride, which means that 0.60 mmol of hydride per mmol of 2-heptanone had been used. After 3 h, the analysis showed 1.505 mmol of residual hydride, which indicates that 0.99 mmol of hydride per mmol of the compound had been consumed. After 6 h, the analysis showed no difference in the residual hydride. These results are summarized in Table 2.

General Procedure for Stereoselectivity Study. The reduction of 2-methylcyclohexanone is described here as representative. To a 25-ml vial capped by a rubber septum was added 1.2 ml of a solution of ThxBHBr·SMe$_2$ in methylene chloride (4 mmol in hydride). The vial was kept at -23°C with the aid of a cooling bath. To this was added 1 ml

of a 2 M 2-methylcyclohexanone solution in methylene chloride (at -23°C). The reaction mixture was kept at -23°C for 6 h. It was then hydrolyzed by the addition of 2 ml of methanol, and then treated with 1 ml of 3 N NaOH and 0.5 ml of 30% H$_2$O$_2$. The aqueous layer was saturated with anhydrous potassium carbonate, and the organic layer was subjected to GC analysis. The results are summarized in Table 3.

References

1. H. C. Brown, B. Nazer, J. S. Cha, and J. A. Sikorski, *J. Org. Chem.*, **51**, 5264 (1986).
2. (a) H. C. Brown, J. S. Cha, B. Nazer, and N. M. Yoon, *J. Am. Chem. Soc.*, **106**, 8001 (1984). (b) H. C. Brown, J. S. Cha, N. M. Yoon, and B. Nazer, *J. Org. Chem.*, **52**, (1987), in press.
3. H. C. Brown, A. K. Mandal, and S. U. Kulkarni, *J. Org. Chem.*, **42**, 1392 (1977).
4. K. Kinberges and W. Siebert, *Z. Naturforsch., Teil B*, **30**, 55 (1975).
5. H. C. Brown, G. W. Kramer, and M. M. Midland, "Organic Syntheses *via* Boranes," Wiley-Interscience, New York, 1975.
6. (a) J. S. Cha, J. E. Kim, S. Y. Oh, J. C. Lee, and K. W. Lee, *Tetrahedron Lett.*, 2389 (1987). (b) J. S. Cha, J. E. Kim, and K. W. Lee, *J. Org. Chem.* (1987) in press.
7. J. S. Cha, S. Y. Oh, and J. E. Kim, *Bull. Korean Chem. Soc.*, **8**, 301 (1987).

Non-Newtonian Intrinsic Viscosities of Biopolymeric and Nonbiopolymeric Solutions (I)

Chun Hag Jang, Jong Ryul Kim, and Taikyue Ree*

Department of Chemistry, Korea Advanced Institute of Science and Technology. Seoul 131. Received April 20, 1987

Experimental results for viscous flow of poly (γ-methyl L-glutamate) solutions have been published elsewhere. The data of $[\eta]^f/[\eta]^o$ are expressed by the following equation,

$$\frac{[\eta]^f}{[\eta]^o}=1-\frac{A}{[\eta]^o}\{1-\frac{\sinh^{-1}[\beta_2\,(f/\eta_0)\,\exp(-c_2 f^2/\eta_0^2 kT)]}{\beta_2 f/\eta_0}\} \quad (A1)$$

where $[\eta]^f$ and $[\eta]^o$ are the intrinsic viscosity at shear stress f and zero, respectively, $A=\lim_{c\to0}[(1/C)(x_2/\alpha_2)(\beta_2/\eta_0)]$, η_0 viscosity of the solvent, β_2 is the relaxation time of flow unit 2, c_2 is a constant related to the elasticity of flow unit 2. The theoretical derivation of Eq.(A1) is given in the text. The experimental curves of $[\eta]^f/[\eta]^o$ vs. log f are compared with the theoretical curves calculated from Eq.(A1) with good results. Eq.(A1) is also applied to non-biopolymeric solutions, and it was found that in the latter case $c_2=0$. The reason for this is explained in the text. The problems related to non-Newtonian flows are discussed.

Introduction

Some theoretical treatments of the dimensional properties of polypeptides in helix-coil transition region were given in our previous papers,[1,2] and the experimental results on intrinsic viscosities of poly(γ-methyl L-glutamate) (PMLG)

solutions were reported elsewhere.[3] In this paper, an equation is derived by using the Ree-Eyring theory of viscosity,[4] which is based on the absolute reaction rate theory, and was successfully applied to polymer solutions, polymer melts,[4] suspension systems,[5] metals, alloys,[6,7] thixotropic and dilatant systems.[8a,b,c] The newly derived equation is applied to

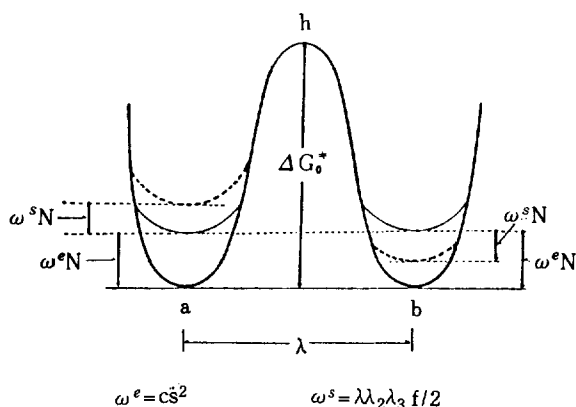$$\omega^e = c\dot{s}^2 \qquad\qquad \omega^s = \lambda\lambda_2\lambda_3\,f/2$$

Figure 1. Energy barrier for flow.

the experimental data[3] of intrinsic viscosities of polypeptide solutions in the helix-coil transition region and to the data for non-biopolymeric solutions.[9] The comparison of the two cases yields a strong support for the newly derived equation.

Theory

The energy barrier curve for flow is represented by a symmetric curve ahb shown in Figure 1. A flow unit lies in the energy minimum position a or b when there is no shear stress f. Under shear stress f, however, the energy of the unit increases by $\omega^e N$ in position a as well as in position b, where N is Avogadro number, and $\omega^e = c\dot{s}^2$ which arises because of the elasticity of the flow unit. There is another increase $\omega^s N$, in the energy of the unit in position a whereas it decreases by $\omega^s N$ in position b where $\omega^s = \lambda_2\lambda_3\lambda f /2$, λ_2, λ_3 and λ being the molecular dimensions appearing in Eyring's flow equation.[10,11] (see Figure 1) The nature of ω^e and ω^s will be considered later.

The activation free energy for forward flow ΔG_f^* and that of backward flow ΔG_b^* are represented, respectively, by

$$\Delta G_f^* = \Delta G_0^* - \omega^e N - \lambda\lambda_2\lambda_3 f N/2$$

and

$$\Delta G_b^* = \Delta G_0^* - \omega^e N + \lambda\lambda_2\lambda_3 f N/2$$

The net rate of flow r is then expressed by the following equation,

$$r = \lambda\,(k_f - k_b) = \lambda\frac{kT}{h}\,[\exp(-\frac{\Delta G_f^*}{RT}) - \exp(-\frac{\Delta G_b^*}{RT})]$$

where k_f and k_b are the rate constant for the forward and the backward jumping, respectively, and λ is the distance between two successive equilibrium positions (Figure 1).

From the above equation, the rate of shear $\dot{s}$ = r/λ_1 is given by

$$s = \frac{\lambda}{\lambda_1}\,\frac{kT}{h}\,\exp[\frac{-(\Delta G_0^* - \omega^e N)}{RT}]\,[\exp(\frac{\omega^s}{kT}) - \exp(-\frac{\omega^s}{kT})]$$

$$= \beta^{-1}\exp(\frac{\omega^e}{kT})\,\sinh(\frac{\lambda\lambda_2\lambda_3 f/2}{kT}) \qquad (1)$$

where λ_1 is the distance between two successive flow layers, β is proportional to the relaxation time of the flow unit, and is expressed by

$$\beta = [2\frac{\lambda}{\lambda_1}\,\frac{kT}{h}\exp(\frac{-\Delta G_0^*}{RT})]^{-1} = (2\frac{\lambda}{\lambda_1}k_0)^{-1} \qquad (1a)$$

The k_0 in Eq.(1a) represents the following quantity:

$$k_0 = \frac{kT}{h}\,\exp(\frac{-\Delta G_0^*}{RT}) \qquad (1b)$$

i.e., k_0 is the rate constant of jumping when there is no shear stress.

Equation (1) is rewritten as

$$\frac{\lambda\lambda_2\lambda_3 f/2}{kT} = \sinh^{-1}[\beta\,\dot{s}\exp(\frac{-\omega^e}{kT})] = \alpha f \qquad (2)$$

where $\alpha = \lambda\lambda_2\lambda_3/2\,KT$, and α^{-1} is proportional to the shear modulus of the flow unit. The relationship between stress f and shear rate $\dot{s}$ for the jth flow unit is obtained from Eq.(2),

$$f_i = \frac{1}{\alpha_i}\,\sinh^{-1}[\beta_i\,s\,\exp(\frac{-\omega^e}{kT})] \qquad (3)$$

where f_i is the shear strees acting on flow unit j, α_j = $(\lambda\lambda_2\lambda_3/2kT)_j$ and β_j = $[(\lambda/\lambda_1)2k_0]_j^{-1}$. We assume that there are three kinds of flow units: solvent unit 0, Newtonian unit 1 and non-Newtonian unit 2. Thus,

$$f = \sum_{i=0}^{12} x_i f_i = x_0 f_0 + x_1 f_1 + x_2 f_2 \qquad (4)$$

where x_j is the fraction of the area occupied by the jth kind of flow units, and

$$f_0 = \frac{1}{\alpha_0}\,\beta_0 s$$

$$f_1 = \frac{1}{\alpha_1}\,\beta_1 s$$

and

$$f_2 = \frac{1}{\alpha_2}\,\sinh^{-1}[\beta_2 s\,\exp(\frac{-\omega^e}{kT})]$$

i.e., in Eq.(4), units 0 and 1 are Newtonian, that is, $\sinh^{-1}\beta_1 s$ $\simeq \beta_1\dot{s}$, and $\omega_0^e = \omega_1^e = 0$ since the Newtonian units have no elasticity. Thus, Eq.(4) becomes,

$$f = \frac{x_0}{\alpha_0}\,\beta_0\dot{s} + \frac{x_1}{\alpha_1}\,\beta_1\dot{s} + \frac{x_2}{\alpha_2}\,\sinh^{-1}[\beta_2\dot{s}\,\exp(\frac{-\omega^e}{kT})] \qquad (4a)$$

The viscosity η and specific viscosity η_{sp} of the flow system are given by the following equations, respectively,

$$\eta = \frac{f}{s} = \frac{x_0}{\alpha_0}\,\beta_0 + \frac{x_1}{\alpha_1}\,\beta_1 + \frac{x_2}{\alpha_2}\,\beta_2\,\frac{\sinh^{-1}[\beta_2\dot{s}\,\exp(\frac{-\omega^e}{kT})]}{\beta_2\dot{s}} \qquad (4b)$$

and

$$\eta_{sp} = \eta_r - 1 = (x_0 + \frac{x_1\beta_1}{\alpha_1\eta_0} - 1) + \frac{x_2\beta_2}{\beta_2\eta_0}\frac{\sinh^{-1}[\beta_2\dot{s}\,\exp(\frac{-\omega^e}{kT})]}{\beta_2\dot{s}} \qquad (4c)$$

where $\beta_0/\alpha_0 = \eta_0$ is the solvent viscosity and $\eta_r\,(=\eta/\eta_0)$ is the relative viscosity. Thus the intrinsic viscosity $[\eta]$ $[= \lim_{c\to 0}(\eta_{sp}/C)$, C = concentration] is represented by,

$$[\eta] = \lim_{c\to 0}\frac{1}{C}\,(x_0 + \frac{x_1\beta_1}{\alpha_1\eta_0} - 1 + \frac{x_2\beta_2}{\alpha_2\eta_0})$$

$$- \lim_{c\to 0}\frac{1}{C}\,\frac{x_2\beta_2}{\alpha_2\eta_0}\{1 - \frac{\sinh^{-1}[\beta_2\dot{s}\,\exp(\frac{-\omega_2^e}{kT})]}{\beta_2\dot{s}}\}$$

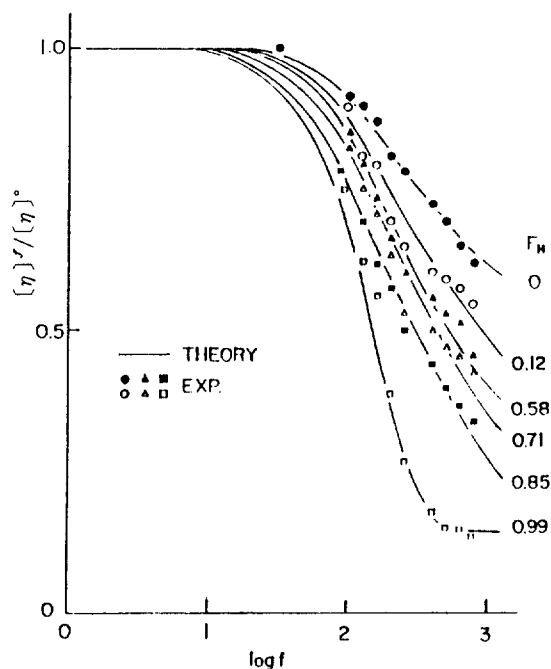$$= [\eta]^0 - A\{1 - \frac{\sinh^{-1}[\beta_2\dot{s}\,\exp(\frac{-\omega_2^e}{kT})]}{\beta_2\dot{s}}\} \qquad (5)$$

Figure 2. Flow curves of poly (γ-methyl L-glutamate) (PMLG) solusions at 25°C.

where

$$A = \lim_{c \to 0} \frac{1}{C} \left(\frac{x_2 \beta_2}{\alpha_2 \eta_0} \right) \tag{5a}$$

and

$$[\eta]^\circ = \lim_{c \to 0} \frac{1}{C} \left(x_0 + \frac{x_1 \beta_1}{\alpha_1 \eta_0} - 1 + \frac{x_2 \beta_2}{\alpha_2 \eta_0} \right) \tag{5b}$$

$[\eta]^\circ$ being the intrinsic viscosity at f → 0. By rearranging Eq.(5), one obtains,

$$\frac{[\eta]^f}{[\eta]^\circ} = 1 - \frac{A}{[\eta]^\circ} \left\{ 1 - \frac{\sinh^{-1} [\beta_2 \dot{s} \exp(\frac{-\omega_2^e}{kT})]}{\beta_2 \dot{s}} \right\} \tag{6}$$

Here we consider the significance of ω_2^e. Unit 2 is a non-Newtonian unit having an elasticity due to molecular chain. Let G be the elasticity constant of the chain. When stress f acts on the chain, an elastic energy ω_2^e is stored on the chain which is represented by the following equation:

$$\omega_2^e = \int_0^{s_c} G s ds = G \frac{s_c^2}{2} \tag{7}$$

where s_c is the critical strain at which the flow unit 2 jumps into the next equilibrium position. The s_c can be expressed by

$$s_c = a \frac{\dot{s}}{k_2}$$

where k_2 in the jumping frequency of the flow unit, and a is proportionality constant. Thus,

$$\omega_2^e = \frac{G}{2} \left(a \frac{\dot{s}}{k_2} \right)^2 = c_2 \dot{s}^2 \tag{8}$$

where c_2 is another proportionality constant which is equal to $(G/2)(a/k_2)^2$. Eq.(8) is originally derived by Hahn, Ree and Eyring,[8a] and successfully used to explain thixotropy and dilatancy phenomena.[8a,b,c]

Table 1[a]. Flow Parameters of PMLG with Various F_H at 25°C

F_H	$[\eta]^\circ$ (dl/g)	A (dl/g)	$\beta_2 10^4$ (sec)	$c_2 10_{22}$ (erg sec^2)	η_0 (cp)
0	1.142	0.58	8.63	0	6.164[b]
0.12	1.204	0.78	10.65	1.432	7.375
0.58	1.421	0.92	12.46	6.873	7.764
0.71	1.493	0.98	19.30	15.11	9.490
0.85	1.741	1.27	23.31	17.62	10.34
0.99	2.680	2.28	25.62	172.0	12.33[c]

[a] In this table $[\eta]^O$ and η_O are experimentally determined values, and A, β_2 and c_2 values are those determined by a non-linear regression method. The molecular weight of the sample $\overline{M}_w = 72{,}000$. We assumed that $[\eta]^O = [\eta]$ (at $\Delta P = O$). [b] Viscosity of dichloroacetic acid (DCA) at 25°C. [c] Viscosity of metacresol (MC) at 25°C. The other η_O's are the viscosities of the mixed solvents of DCA and MC, which yield the PMLG having the F_H shown in the first column.

Next the work $\omega^s = \lambda \lambda_2 \lambda_3 f/2$ is considered. This function is originally introduced by Eyring,[10a,b,11] and is well known in the field of rheology. It is caused by the fact that the flow unit exists in the flow potential field which helps the flow while it retards the reverse flow. Thus ω_2^s is quite different from ω_2^e in its origin. The Hahn-Ree-Eyring theory of thixotropy[8a] is based on the fact that if ω^e is large enough, the flow unit is destroyed.

In Eq.(6), $\dot{s}$ is replaced by f/η_c since all the flow units in the system flow with equal shear-rate $\dot{s}$ and since we are treating a very dilute solution (lim C → 0), i.e., $\eta_0 \simeq f_0/\dot{s} = f/\dot{s}$. Thus, Eq.(6) is rewritten as

$$\frac{[\eta]^f}{[\eta]^\circ} = 1 - \frac{A}{[\eta]^\circ} \left\{ 1 - \frac{\sinh^{-1} [\beta_2 (f/\eta_0) \exp(\frac{-c_2 f^2/\eta_0^2}{kT})]}{\beta_2 f/\eta_0} \right\} \tag{9}$$

where ω_2^e in Eq.(6) is substituted by Eq.(8). The superscript f is attached to $[\eta]$ to emphasize that the latter is the $[\eta]$ at f.

Applications

(A) Flow Curves of Poly(γ-methyl L-glutamate).

The experimental flow curves,[3] $[([\eta]^f/[\eta]^o)$ vs. log f], for poly(γ-methyl L-glutamate) are shown in Figure 2, where F_H (the helix content in the PMLG) is shown on each curve, and shear stress f is expressed in the units of dyn/cm^2, where f is given by

$$f = (\Delta P + \rho g h)/(R/2L) \tag{10}$$

ΔP = external pressure applied to the viscometer, ρ = density of the sample liquid, h = the height of the liquid column in the viscometer, g = gravitational constant, R and L are the radius and the length of the capillary of the viscometer, respectively. From Figure 2, one notes that the viscosity decreases with increasing stress, i.e., that the flow phenomena are non-Newtonian.

We apply Eq.(9) to the flow curves of Figure 2, the parameters appearing in Eq.(9) are determined by a non-linear regression method,[12] and are summerized in Table 1. The full curves are those calculated from Eq.(9) by using the parametric values shown in Table 1. One notes that the theoretical curves express well the experimental data. [Note:
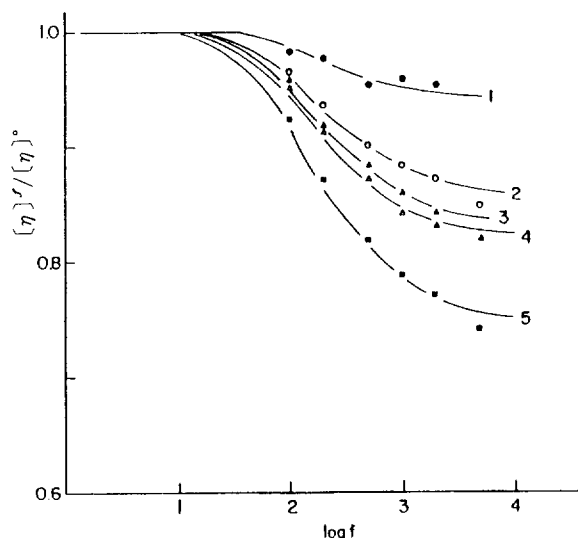
Figure 3. Flow curves of polyisobutylene dissolved in various solvents at 25°C.[9] More details of the curves are given in Table 2.
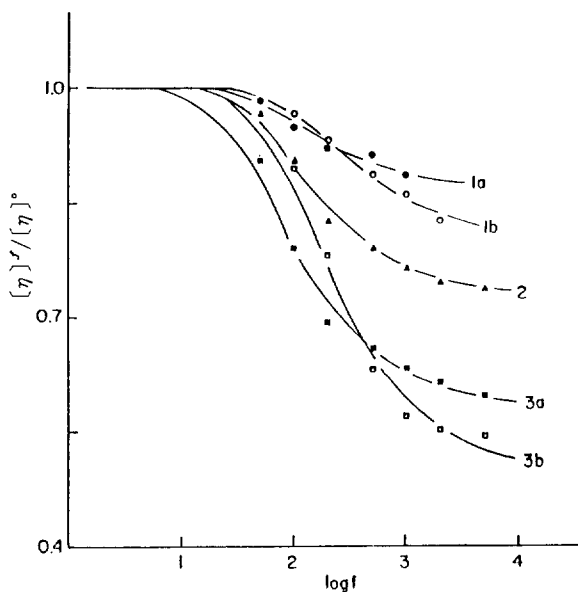

Figure 4. Flow curves of polystyrene disolved in various solvents at 25°C.[9] More details of the curves are given in Table 3.

the theoretical curve of $F_H = 0$ in Figure 2 was calculated from Eq.(9) with $c_2 = 0$; we use in this paper $F_H = 0$ as a

Table 2a. Intrinsic Viscosities and Parameters of Polyisobutylene in Various Solvents at 25°C

sample[b] No.	$\overline{M}_W \cdot 10^{-6}$	$[\eta]^o$ (dl/g)	α_f	A (dl/g)	β_2/η_o (cm²/dyn)	C_2 (erg sec²)	Solvent
1	1.59	1.50	1.94	0.093	0.017	0	Benzene
2	1.59	2.90	2.50	0.42	0.021	0	Decalin
3	1.59	3.87	2.74	0.65	0.023	0	$C_6H_5C_2H_5$
4	1.59	4.40	2.88	0.79	0.025	0	Isooctene
5	4.85	6.35	3.22	1.61	0.026	0	C_6H_{12}

a $[\eta]^o$, $\overline{M}_w$ and α_f (extension factor) are experimental data of Passaglia *et al.*[9]. A, β_2/η_o and c_2 are those obtained by a nonlinear regression method. *b* The sample numbers 1 to 5 indicate also the order of the solubility power of the solvents from poor to the best. The order accords also with that of the α_f.

synonym of $c_2 = 0$.

We also applied Eq.(9) to the flow curves of poly(γ-benzyl L-glutamate) (PBLG),[13] with good result, but the details are reserved for a future publication.

(B) Flow Curves of Non-Biopolymeric Solutions

Equation (9) was applied to the flow curves of non-biopolymeric solutions, e.g., polyisobutylene (Figure 3) and polystyrene (Figure 4). The experimental points in Figure 3 and 4 are the data obtained by Passaglia *et al.*[9] More details of the curves are shown in Tables 2 and 3. By applying Eq. (9) with $c_2 = 0$, we obtained the values of the parameters appearing in Eq.(9), and summarized in Tables 2 and 3. The full curves in Figures 3 and 4 are those calculated from Eq.(9) with $c_2 = 0$ by using the parametric values in Tables 2 and 3, respectively. One notes that the theory and experiment agree very well. From Tables 2 and 3, it is noticed that for the organic polymers the elasticity factor c_2 in Eq.(9) is zero. The reason will be mentioned in the next section.

Results and Discussion

**(A) The c_2 Factors for Biopolymers and Nonbiopolymers**

We found in the above that the elasticity factor c_2 for biopolymers plays a remarkable role in the flows while $c_2 = 0$ for the nonbiopolymeric solutions, polyisobutylene and polystylene. The reason will be considered below.

Biopolymers, e.g., poly(γ-methyl L-glutamate) and poly(γ-benzyl L-glutamate), have a peptide chain (-CO-NH-CHR-)$_n$, which makes a helix, the intramolecular hydrogen bonds formed in the peptide chain help the helix formation.[14a] For

Table 3.a Intrinsic Viscosities and Parameters of Polystyrene in Various Solvents at 25°C

sample No.	$\overline{M}_w 10^{-6}$	$[\eta]^o$ (dl/g)	α_f	A (A/[η]^o) (dl/g)	β_2/η_o (cm²/dyn)	c_2 (erg sec²)	solvents
1a	3.22	1.35	2.35[b]	0.17(0.126)[c]	0.027	0	C_6H_{12}/CCl_4 (0.869/0.131)
1b	2.83	2.00	2.74	0.39(0.195)	0.014	0	$C_6H_5CH_3/n\text{-}C_7H_{16}$ (0.476/0.524)
2	2.82	4.40	3.57	1.20(0.273)	0.019	0	Toluene
3a	1.89	4.60	3.87	1.93(0.420)	0.043	0	Tetralin
3b	2.83	5.10	3.74	2.56(0.502)	0.020	0	Tetralin

a $[\eta]^o$, $\overline{M}_w$ and α_f are experimental data.[9] A,β_2/η_o and c_2 are those determined by a non-linear regression method. *b* The order of α_f indicates also the solubility power of the solvents from poor to the best. *c* The parenthesized data indicate the values of A/[η]^o which is dimension less.
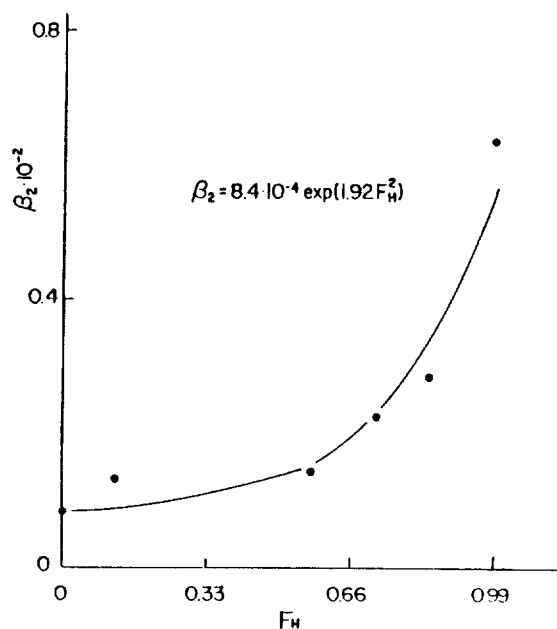
Figure 5. Relaxation time β_2 vs. helix content F_H. The dots represent the β_2 values from Table 1. Full curve is represented by Eq. (11).

the non-biopolymeric solutions such as polyisobutylene and polystylene, the situation is quite different, they form random coil structure,[14b] thus they do not show the elasticity nature. This is the reason for $c_2 = 0$ for the organic polymers.

(B) Dependence of β_2 on F_H

We plot β_2 values in Table 1 against F_H in Figure 5, the curve is represented by

$$\beta_2 = 8.4 \cdot 10^{-4} \exp(1.92 \; F_H^2) \tag{11}$$

As mentioned previously [see Eq.(1a)],

$$\beta_2 = \frac{\lambda_1}{\lambda} \frac{h}{2kT} \exp[\frac{(\Delta G_0^*)_2}{RT}] \tag{11a}$$

where $(\Delta G_0^*)_2$ signifys the activation free energy for unit 2 at $f = 0$ [see Eq.(1b)]. By equating Eqs.(11) and (11a), we obtain,

$$8.4 \cdot 10^{-4} \exp(1.92 \; F_H^2) = \frac{\lambda_1}{\lambda} \frac{h}{2kT} \exp[\frac{(\Delta G_0^*)_2}{RT}]$$

from which the $(\Delta G_0^*)_2$ is obtained as

$$\frac{(\Delta G_0^*)_2}{RT} = 1.92 \; F_H^2 + \ln[(8.4 \cdot 10^{-4}) \frac{\lambda}{\lambda_1} \frac{2kT}{h}]$$

we assume $\lambda_1/\lambda \simeq 1$ and calculate $(\Delta G_0^*)_2$ at T = 298K and $F_H = 1$. Then $(\Delta G_0^*)_2 = 14.9$ kcal is obtained,. Similarly, $(\Delta G_0^*)_2 = 14.3$ kcal was calculated at $F_H = 0.5$, both values of $(\Delta G_0^*)_2$ seem to be very reasonable, since according to our experiences, for processes occuring at normal temperature and pressure ΔG_0^* rarely exceed 40 kcal.

(C) Correction Factors in Non-Newtonian Flow

(1) *Rabinowitsch Correction.* The rate of shear s was obtained from the volume-flow rate Q(V/t = 5.80 cm³/t) by $\dot{s} = 4Q/\pi\gamma^3$ which must be corrected by Rabinowitsch equation[15] to obtain the true rate of shear $\dot{s}_{tr}$ at wall, *i.e.*,

$$\dot{s}_{tr} = \frac{\dot{s}}{4} (\frac{d \log \dot{s}}{d \log f} + 3) = \frac{\dot{s}}{4} (n + 3) \tag{12}$$

where f is the shear stress at wall, and is given by Eq.(10).

In order to obtain the factor n in Eq.(12), we plotted our experimental data of log $\dot{s}$ against log f, and obtained the result that n = 1 for all the cases of F_H in dilute solutions. Thus, we found that our experimental rate of shear $\dot{s}$ is nearly equal to $\dot{s}_{tr}$ [see Eq.(12)]. Accordingly, we use in this paper s for $\dot{s}_{tr}$.

(2) *Hagenbach correction.* For shear stress f, the correction for the kinetic energy and the "end" effects must be considered by viscometry by a capillary flow. The Hagen-Poisseuille equation (also known as Hagenbach-Couette equation), which corrects both effects, may be written as[16]

$$\eta = \frac{\pi R^4 P}{8Q (L + n'R)} - \frac{m'\rho Q}{8\pi (L + n'R)} \tag{13}$$

where n' is a correction factor for the end-effect, and m' is a proportionality constant for correcting the kinectic energy. The value of m' may depend on the apparatuses and the liquids used, however, various authors reported the values of m' changing from 0.55 to 1.55.[16] For the end-effect correction factor n', it becomes unimportant at low shear stresses $< 10^4$ dyn/cm² and for the tubes for which L/R > 100.[9] Since in our experiment, f $< 10^3$ dyn/cm² and L/R = 293.65, we can assumed that n' = 0. Then we can estimate the second term on the right of Eq.(13) by assuming m' = 1 which is very reasonable (see above).

We consider the case of PMLG in metacresol (MC) solvent in which the F_H of PMLG is equal to 0.99 (see Figure 2). We apply Eq.(13) to this case where ΔP = 6.0 psi. The P in Eq.(13) is P = ΔP + hρg where h = 13.5 cm, thus P = 4.27. 10^5 dyn/cm², ρ being 1.034. By using the data Q = V/t = 5.8/70.13 = 0.0827 cm³/sec, L = 9.25 cm and R = 0.0315 cm, the first and second terms on the right of Eq.(13) are calculated at 0.216 and 3.66 × 10⁻⁴ poise, respectively, *i.e.*, the correction term (the second term) is negligibly small compared to the first term, the Newtonian viscosity term. Similar calculation were performed in other cases of different solvents and ΔP, and similar results were obtained always, *i.e.*, the correction term is negligible in our experiment.

From the results obtained by the calculations of Eq.(12) and (13), the rate of shear $\dot{s}$ and shear stress f (both at the wall) can be represented by $\dot{s} = 4Q/\pi r^3$ and f = PR/2L, *i.e.*, any correction for the non-Newtonian flow is not necessary. Then, one would wonder why the non-Newtonian flow nature appears in the experimental curves of Figure 2 while it does not in the Rabinowitsch equation. We consider the reason for this question below.

In the Rabinowitsch equation, the correction factor n is determined by the shape of the curves of log $\dot{s}$ vs. log f, and we found n = 1 as already mentioned, *i.e.*, n is determined by a double lograithmic plot. In Figure 2, however, $[\eta]^f/[\eta]^o$ is plotted vs. log f, *i.e.*, by a semilograithmic plot, thus the change in $[\eta]^f/[\eta]^o$ vs log f appeares more precisely than the double lograithmic plots. This is the reason for the appearance of non-Newtonian character in the plots of $[\eta]^f/[\eta]^o$ vs. log f (Figure 2) while the Rabinowitsch equation Eq.(12) and the Hagenbach equation (13) show Newtonian character.

(3) *Turbulence Effect.* Generally at high shear rates, tur bulent flow occurs. Thus, it will be interesting to see whether it will occur in our case or not. We calculate the Reynold number Re which is given by the following equation:[17]

$$Re = \frac{2\rho}{\eta} \frac{Q}{\pi R} \tag{14}$$

We apply Eq.(14) to the solution of PMLG in MC, the concentration of which being 1.7 g/dl, and obtained Re = 7.97 by using the data, R = 0.0135 cm, Q = 0.0827 cm³/sec, ρ = 1.034 g/cm³, and the Newtonian viscosity of the solution η = 0.216 poise.

According to the literature[17b] laminar flow occurs whenever Re < 1000. Comparing our value of Re = 7.97 to the literature value, we conclude that turbulent flow does not occur in our experiment.

(D) Remarks on Non-biopolymeric Solutions

In the above discussions, we are mainly concerned with biopolymeric solutions. Now we are in a position to discuss our results on non-biopolymeric solutions. Most of the problems, however, will be reserved for a future publication except for the results shown in Figure 3 where the crossing of flow curves appeared.

As one notes from Figure 4, the curves 1a and 1b, and curves 3a and 3b cross with each other. The crossing occurs by the interrelation between the parameters β_2/η_0, $[\eta]°$ and $A/[\eta]°$ of the curves. See, for example, curves 3a and 3b: for β_2/η_0, curve 3a > curve 3b (Table 3), and the former drops from the line of $[\eta]'/[\eta]° = 1$ at the lower value of f while the reverse is true for curve 3b. The reason is considered below.

To the polystyrene solutions (curve 3a and 3b), Eq.(9) is applied where c_2 is zero as mentioned previously. When f is very small, the braced term in Eq.(9) changes in the following way:

$$\lim_{f \to 0} \left\{ 1 - \frac{\sinh^{-1}\beta_2 f/\eta_0}{\beta_2 f/\eta_0} \right\} \to \left\{ 1 - \frac{\beta_2 f/\eta_0}{\beta_2 f/\eta_0} \right\} = 0 \qquad (15)$$

thus $[\eta]'/[\eta]° \to 1$ (see Eq.(9)). If f increases, the above relation (i.e., $\sinh^{-1}\beta_2 f/\eta_0 \fallingdotseq \beta_2 f/\eta_0$) does not hold, thus the value of $[\eta]'/[\eta]°$ drops from unity. Stress f^c, at which $[\eta]'/[\eta]°$ drops from unity, changes by the value of β_2/η_0, i.e., β_2/η_0 is the smaller, the f^c becomes the larger, vice versa. (see Figure 4)

Next we consider the limiting value of the braced term in Eq.(9) at $f \to \infty$:

$$\lim_{f \to \infty} \left\{ 1 - \frac{\sinh^{-1}\beta_2 f/\eta_0}{\beta_2 f/\eta_0} \right\} = \lim_{f \to \infty} \left\{ 1 - \frac{\ln (2\beta_2 f/\eta_0)}{\beta_2 f/\eta_0} \right\} \to 1 \ (15a)$$

Thus Eq.(9) becomes

$$\frac{[\eta]'}{[\eta]°} = 1 - \frac{A}{[\eta]°} \equiv L \qquad (16)$$

Let the limiting value of $[\eta]'/[\eta]°$ be L. Then by using Table 3 and Eq.(16) the L values of the cases for curve 3a and 3b are calculated, respectively.

$$L_{3a} = 1 - 0.420 = 0.580$$
$$L_{3b} = 1 - 0.502 = 0.498$$

Thus curve 3a, for which β_2/η_0 = 0.043, has higher value of L while curve 3b, for which β_2/η_0 = 0.020, has lower L; as a result, the curves 3a and 3b cross at a point (see Figure 4).

Concerning the crossing of curves 1a and 1b, the situation is exactly equal to the case of curves 3a and 3b. Thus it need not any special comments.

(E) The Nature of Flow Units

It will be advisable to clarify the nature of flow units considered in this paper although fragmental explanation were given in some our previous papers. See, for example,
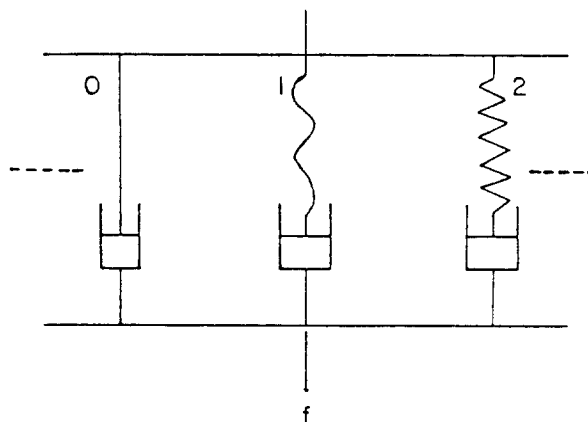
Figure 6. Mechanical model of the flow system composed of generalized Maxwell moldel.

reference 4b.

Macromolecules, in general, moves by a segmental motion, the size of segments (the number of chain atoms z per segment) was estimated in various ways for various cases.[18] For the present case, however, Fox *et al.*'s estimation[18b] seems to be most suitable. According to these authors z is no more larger than 5 for poly(n-paraffins), while for poly-isobutylene and polystyrene z is less than 10. We treated in this paper the polymeric systems in which the number of repeating units $\overline{N}_w$ is changing from 600(PMLG) to 85000 (PIB). According to Fox *et al.*'s estimation, the number of flow units is estimated as 200 per molecule (at least) in biopolymeric systems, and as 500 per molecule (at least) in non-biopolymeric systems. Some of these flow units are entangled with each other whereas the others are in disentangled states. Under shear stress, these flow units move, the disentangled flow units moving somewhat freely, i.e., as Newtonian units, while the entangled units flowing with some difficulty, i.e., as non-Newtonian units.

Our model of the polymeric flow systems is represented by a mechanic model in which Maxwell elements connected in parallel as shown in Figure 6. Units 0 and 1, represent the solvent and the Newtonian units, respectively, while unit 2 represents the non-Newtonian units with elastic spring. The stress acting on the flow units f_0, f_1 and f_2 are different, i.c., $f_0 < f_1 < f_2$ whereas the rates of shear are equal, i.e., $s_0 = s_1 = s_2$. These constraints are impressed in a high molecular polymeric system by the fact that the corresponding flow segments (or units) are connected to the backbone chain. The solvent molecules are also attatched to the backbone chain, thus the attached solvent molecules may be treated as an "0" type element in Figure 6.

Previously we mentioned that the peptide chain (-NH-CH(R)-CO-)$_n$ in PMLG (or PBLG) makes a helix chain having elasticity. The work-done ω_i^e (= $c_2 s^2$) [Eq.(8)] is due to the spring, and helps the jumping over the energy barier (i.e., reducing the barrier height). The molecular explanation for this phenomenon is as follows: by the extension of the helix, the included solvent molecules in the helix are expelled from the helix-chain segment making it easier to flow, otherwise the included solvent molecules move with the helix element making the movement harder. In the mechanical model (Figure 6), the abovementioned phenomenon corresponds to the fact that the work ω_i^e is used for loosening the dashpot.

It was found that PMLG F_H = 0 and c_2 = 0 in dichl-

oroacetic acid (DCA) (See Table 1). This is explained as follows: in DCA the entanglement juncture of PMLG (or PBLG) becomes loose, thus the peptide chain looses the elasticity and the helixity at the same time (*i.e.*, $c_2 = 0$ and $F_H = 0$).

We also found that $c_2 = 0$ for polyisobutylene, polystyrene, etc. (Table 2 and 3). This is due to the fact that the entanglement joints of the non-biopolymeric chains are not tight compared to that helix chains of polypeptides. [Note: it maybe noted that the 2-type non-Newtonian unit can work as a non-Newtonian unit even after attaining the state $c_2 = 0$, since this state signifys, only the state at which the entangled juncture becomes loose.]

References

1. J. R. Kim and T. Ree, *Polym. J.*, **16**, 669 (1984), *ibid.*, **16**, 677 (1984).
2. J. R. Kim and T. Ree, *J. Polym. Sci. Polym. Chem. Ed.*, **23**, 215 (1985).
3. C. H. Jang, J. R. Kim, and T. Ree, *J. Polym. Sci: Polym. Chem. Ed.*, **24**, 3171 (1986).
4. (a) T. Ree and H. Eyring, *J. Appl. Phys.*, **26**, 793, 800 (1955); (b) "Rheology, Theory and Application I," F. R. Eirich, ed., Academic Press, New York, 1958, p. 83-144.
5. A. F. Gabrysh, T. Ree, H. Eyring, D. Makee, and I. Cutler, *Trans, Soc. Rheol.*, **5**, 67 (1961).
6. F. H. Ree, T. Ree, and H. Eyring, *J. Eng. Mech. Div. Proc. Am. Soc. Civ. Engr.*, EMI, 41 (1960).
7. C. H. Jang, C. H. Kim, and T. Ree, *Bull. Korean Chem. Soc.*, **5**, 73 (1984).
8. (a) S. J. Hahn, T. Ree and H. Eyring, *Ind. and Eng.*

Chem., **51**, 856 (1959); (b) D. A. Sohn, E. R. Kim., S. J. Hahn and T. Ree, *Bull. Korean Chem. Soc.*, **7**, 257 (1986); (c) J. H. Bang, E. R. Kim, S. J. Hahn and T. Ree, *ibid.*, **4**, 212 (1983).
9. E. Passaglia, J. T. Yang and N. J. Wegemer, *J. Polym. Sci.*, **47**, 333 (1960).
10. H. Eyring, (a) *J. Chem. Phys.*, **4**, 283 (1936); (b) S. Glasstone, K. J. Laidler and H. Eyring, "The Theory of Rate Processes," McGraw-Hill Co., New York, 1942, pp. 480-484.
11. A. S. Krausz and H. Eyring, "Deformation Kinetics," Jhon Wiley, New York, 1975, pp. 39-45.
12. J. L. Kuester and J. H. Mize, "Optimization Techniques with Fortran," McGraw-Hill Co., New York, 1973, pp. 240-250.
13. J. T. Yang, *J. Am. Chem. Soc.*, **80**, 1783 (1958); **81**, 3902 (1959).
14. (a) L. Stryer, "Biochemistry," W. H. Freeman Co., 1975, p. 29, (b) P. J. Flory, "Statistical Mechanics of Chain Molecules," John Wiley, 1969, p. 40.
15. (a) B. Rabinowitsch, *Z. physik. Chem.*, **A145**, 1 (1929), (b) M. Mooney, *J. Rheol.* **2**, 210 (1931), (c) A. G. Frederickson, "Principle and Application of Rheology," Prentice-Hall, Englewood Cliffs, N.J. (1964), p. 30.
16. S. Oka, "Rheology, Theory and Application III," F. R. Eirich, ed., Academic Press, New York, 1960, p. 17, 25.
17. (a) H. L. Frisch and R. Simha, in "Rheology, Theory and Applications I," F. R. Eirich, ed., Academic Press, New York, 1956, p. 525; (b) B. A. Toms, *ibid.*, II, 1958, p. 475.
18. (a) W. Kausmann and H. Eyring, *J. Am. Chem. Soc.*, **62**, 3113 (1940), (b) T. G. Fox, S. Gratoh and S. Loshack, "Rheology, Theory and Applications, I," F.R. Eirich ed., Academic Press, New York, 1956, p. 487, (c) J.D. Ferry, "Viscoelastic Properties of Polymers," John Wiley, New York, 1961, p. 403-407.

Catalytic Reactions of 3-Phenyl-2-propen-1-ol with Perchloratocarbonylbis (triphenylphosphine) rhodium (I)[†]

Jeonghan Park and Chong Shik Chin*

Department of Chemistry, Sogang University, Seoul 121. Received April 27, 1987

Reaction of Rh (ClO_4) (CO) (PPh_3)$_2$ (**1**) with *trans*-$C_6H_5CH = CHCH_2OH$ (**2**) produces a new cationic rhodium(I) complex, [Rh(*trans*-$C_6H_5CH = CHCHO$) (CO) (PPh_3)$_2$]ClO_4 (**3**) where **2** is coordinated throuth the oxygen atom but not through the olefinic group. At room temperature under nitrogen, complex **1** catalyzes dehydrogenation, hydrogenolysis, and isomerization of **2** to give *trans*-$C_6H_5CH = CHCHO$ (**4**), *trans*-$C_6H_5CH = CHCH_3$ (**5**) and $C_6H_5CH_2CH_2CHO$ (**6**), respectively, and oligomerization of **2** whereas under hydrogen, complex **1** catalyzes hydrogenation of **2** to give $C_6H_5CH_2CH_2CH_2OH$ (**7**) and hydrogenolysis of **2** to **5** which is further hydrogenated to $C_6H_5CH_2CH_2CH_3$ (**8**). The dehydrogenation and hydrogenolysis of **2** with **1** suggest an interaction between the rhodium and the oxygen atom of **2**, whereas the isomerization and hydrogenation of **2** with **1** indicate an interaction between the rhodium and the olefinic system of **2**.

Introduction

Reactions of unsaturated aldehydes[1] and unsaturated

esters[2] with Rh(ClO$_4$)(CO)(PPh$_3$)$_2$ (**1**) produce cationic four-coordinated rhodium(I) complexes, [RhL(CO)(PPh$_3$)$_2$]ClO$_4$ (L=unsaturated aldehydes and unsaturated esters coordinated through oxygen atom but not through the olefinic

---

[†] Dedicated to professor Nung Min Yoon for this 60th birthday.